Dentomaxillofacial Radiology (2013) 42, 20120436

http://dmfr.birjournals.org

TECHNICAL REPORT

Dynamic MRI of the TMJ under physical load

A J Hopfgartner*[,1], O Tymofiyeva[2], P Ehses[1], K Rottner[2], J Boldt[2], E-J Richter[2] and P M Jakob[1]

[1]*Department of Experimental Physics 5, University of Wuerzburg, Wuerzburg, Germany;* [2]*Department of Prosthodontics, University of Wuerzburg, Wuerzburg, Germany*

Objectives: The objective of this study was to examine the kinematics of structures of the temporomandibular joint (TMJ) under physiological load while masticating.
Methods: Radial MRI was chosen as a fast imaging method to dynamically capture the motions of the joint's anatomy. The technique included a golden ratio-based increment angle and a sliding window reconstruction. The measurements were performed on 22 subjects with and without deformation/displacement of the intra-articular disc while they were biting on a cooled caramel toffee.
Results: The reconstructed dynamic images provided sufficient information about the size and localization of the disc as well as the change of the intra-articular distance with and without loading.
Conclusions: The feasibility of the golden ratio-based radial MRI technique to dynamically capture the anatomy of the TMJ under physical load was demonstrated in this initial study.
Dentomaxillofacial Radiology (2013) **42,** 20120436. doi: 10.1259/dmfr.20120436

Cite this article as: Hopfgartner AJ, Tymofiyeva O, Ehses P, Rottner K, Boldt J, Richter E-J, et al. Dynamic MRI of the TMJ under physical load. *Dentomaxillofac Radiol* 2013; **42:** 20120436.

Keywords: magnetic resonance imaging (MRI); temporomandibular joint (TMJ); temporomandibular joint disc

Introduction

The temporomandibular joint (TMJ) can suffer from a number of diseases, which are classified as temporomandibular disorders (TMDs).[1] These are the major reasons for non-dental pain in the orofacial region.[2] While TMD is an umbrella diagnosis[3] originating in different causes, clinical signs and symptoms are similar.

When a patient complains about clicks or pain related to the TMJ while chewing or moving the mandible, it is of interest to determine what happens during motion under masticatory loading that can exert strong forces on the joint.[4–7]

In practice, mandibular motion is commonly tracked using axiography.[8–10] With real-time axiography, a precise picture of the TMJ's motion can be drawn at high resolution in space and time. Unfortunately, this method only allows inferences about the anatomy of the TMJ from the shape of the tracings, which is complex. By contrast, static MRI depicts the anatomical situation of soft tissue and bone, without information on kinematics. Thus, it is of importance to have an appropriate imaging method for visualizing the kinematics of the TMJ's structures in action.

Several imaging techniques have been used for the evaluation of the TMJ. Among them, MRI has advantages over other techniques depicting soft tissue of the TMJ[11–14] while not relying on ionizing radiation. The mechanically and temporally complex motion characteristics of the TMJ with its disc[15,16] present substantial difficulties when using conventional MRI methods to capture articulation kinetics as motion artefacts occur. Past work has been carried out on static MRI acquisition of the TMJ,[17] quasistatic images[18,19] and dynamic[20,21] imaging of the unloaded TMJ. However, to our knowledge, no MR study under masticatory loading has been published.

The purpose of this study was to visualize the kinematics of the TMJ's components under masticatory load. We used radial MRI for a rapid image acquisition to depict the motion of the loaded TMJ. Radial imaging is an

*Correspondence to: Dr A J Hopfgartner, Department of Experimental Physics 5, University of Wuerzburg, Am Hubland, 97074 Wuerzburg, Germany. E-mail: andreas.hopfgartner@physik.uni-wuerzburg.de
Received 3 December 2012; revised 12 August 2013; accepted 19 August 2013

MRI technique that was firstly presented by Lauterbur and Lai.[22] For a closer look on MRI physical principles and sequence design technique, see Haacke et al.[23]

Materials and methods

Subjects

MRI was performed on 22 subjects (mean age 30 years, median 27 years, age span 18–68 years), among them 8 subjects who had been diagnosed beforehand with various TMDs. These included deformation or displacement of the intra-articular disc. Written informed consent was obtained from each subject.

The subjects were examined on a 1.5 T whole-body MRI scanner (MAGNETOM® Avanto 1.5 T; Siemens Medical Solutions, Malvern, PA) using two 4-channel multiarray coils (Noras, Hoechberg, Germany). The measurement set-up is shown in Figure 1. The patients were stabilized with cushions to avoid head motions during the measurement which could result in misaligned image slices or distortions by motion artefacts.

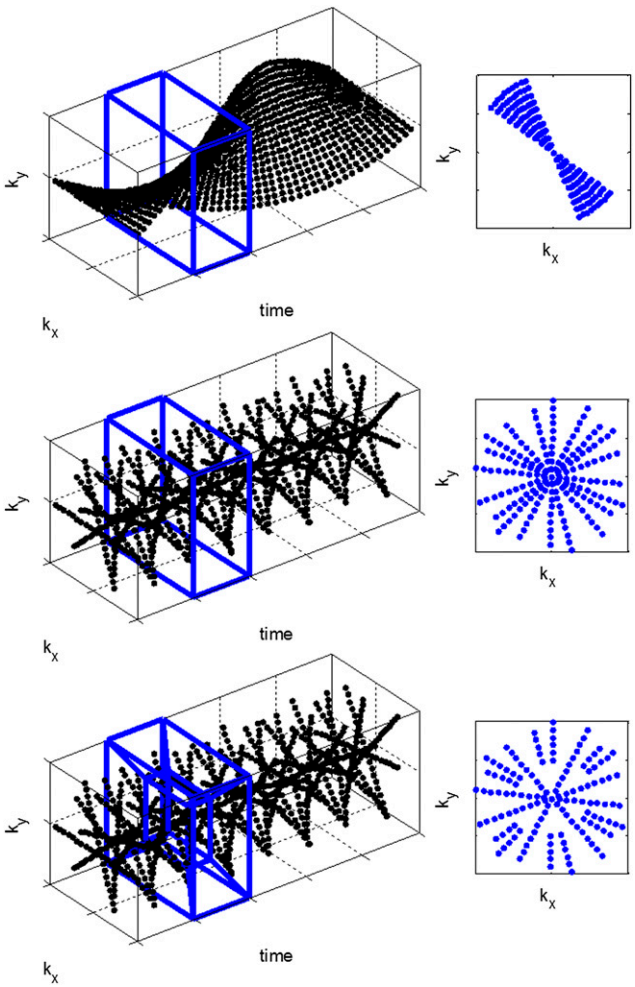

Figure 1 A sliding window reconstruction with linear (top) *vs* golden ratio (middle) radial sampling and the k-space-weighted image contrast filter (bottom) is shown. The box depicts the reconstruction window sliding along time axis over the data set. In the two-dimensional images, the k-space of the reconstruction frame is shown. Big and irregular gaps result in strong artefacts. A linearly filled up k-space demands a rather wide reconstruction window that may in turn result in motion artefacts

MRI protocol

In addition to the standard static measurements (T_1 and T_2 weighted turbo-spin echo multislice sequences), two different kinds of TMJ measurements were performed. The first method consisted of opening and closing of the mouth within 15 s, half for the opening and closing motions. The second method was aimed at analysing the joint, cartilage tissue and the intra-articular space (distance between condyle and fossa) under masticatory loading. The volunteers were instructed to bite once through a chocolate-covered caramel candy (Storck Riesen®; August Storck KG, Berlin, Germany) placed either on one side or on both sides between the maxillary and mandibular molars to produce unilateral or bilateral loading, respectively. To compensate for individual factors, such as tooth shape and strength of the masticatory muscles, the candy was cooled to such an extent that the volunteer could bite through the candy roughly within the acquisition time of 15 s. The candy was placed in the back most posterior position between the right and the left molars to monitor the complete closing motion.

Similar to the MRI parameters as used by Yamada et al,[17] a radial FLASH sequence [echo time (TE) = 3.17/5/12 ms, repetition time (TR) = 15/30 ms, excitation flip angle 8°/11°, in-plane resolution $0.59 \times 0.59\ mm^2$, slice thickness 3 mm, two non-parallel alternatingly measured slices for the right and left TMJ] was adapted and employed for examination of the intra-articular space. The different TE times were used to depict the disc (longer TE) or to increase the signal-to-noise ratio (short TE). Because of the short T_2 of the fibrocartilagenous tissue, the disc yields low signal at long TEs and is delineated in contrast to the surrounding tissues. On the other side, the shorter TE of 5 ms results in a higher contrast between the cortical bone and soft tissue of the intra-articular space.

Radial golden ratio-based dynamic imaging

In MRI, three-dimensional spin density information from inside the body is frequency encoded (see k-space concept[24]) by applying linear magnetic field gradients. Anatomical images are obtained from the acquired raw data set by a Fourier transformation.[25] Typically, classic Cartesian sampling[26] is used in medical MRI because data sets can be easily and quickly calculated. In radial MRI, a trajectory through the k-space equals a spoke that crosses the k-space centre. Continuous radial data acquisition[27] is required for capturing the joint motion. An image reconstruction frame with a dedicated frame width which is optimized for joint motion velocity is laid over the data set [sliding window and k-space-weighted image contrast (KWIC) reconstruction, Figure 2]. Equally distributed and therefore adequate azimuthal profile spacing is indispensable for a flexible

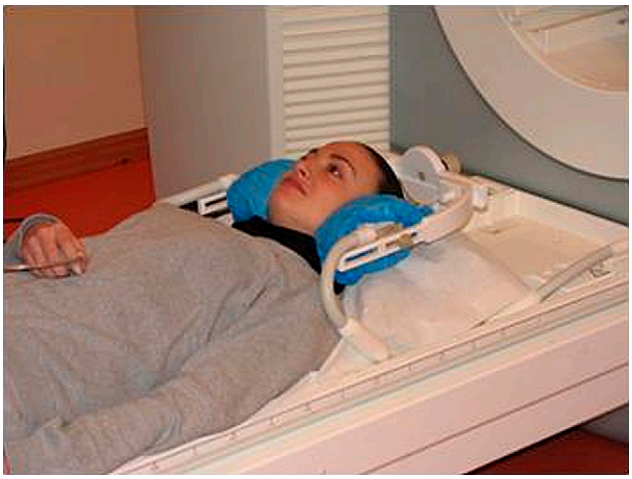

Figure 2 Typical set-up of a temporomandibular joint measurement. The subject is placed between two multichannel coils that do not interfere with the jaw motion. Cushions stabilize the head to prevent motion artefacts and misaligned slices. All measurements were well tolerated by the subjects

reconstruction. The k-space can be filled incrementally, interleaved or by an angle based on the principle of golden ratio.[28] Filling up the frequency space incrementally or interleaved with a narrow angle yields an image with high resolution. Because acquisition time of every single projection requires a certain time, the overall time to completely fill up the frequency space is quite long. If the incremental angle is increased, the density of sampling points, hence the resolution, is lowered. With these techniques, the decision on trading off spatial against temporal resolution must be made before the measurement, requiring *a priori* knowledge about the expected motion kinetics.

By contrast, the golden ratio-based increment angle makes it possible to decide about the reconstruction window parameter after the measurement. The incremental angle amounts to 111.25°.[28] Filling up the frequency space with projections that include the golden angle guarantees that two projections never overlap and that projections are spread uniformly over the entire frequency space. This enables a flexible reconstruction without *a priori* knowledge because a reconstruction window can contain an arbitrary number of projections.

As the fast Fourier transform[29] computation expects the data to be received in a lattice form, the radial data points have to be regridded.[30] In this special case, a non-uniform fast Fourier transform designed by Fessler[31] was used.

The sliding window reconstruction[27] is a view-sharing technique. A certain number of adjacent projections are pooled to form a reconstruction window (Figure 2). This window slides along all the acquainted data points. The image quality and the temporal resolution of the motion depend on the width and the jump width of this reconstruction window. If, to diminish the temporal blurring artefacts, the number of spokes for one frame is decreased, one runs the risk of undersampling which shows up in streaking artefacts in the image. One can overcome this by filling the growing gaps in outer k-space with data points farther from the frame centre (KWIC filter).[32,33] The filter was originally designed for dynamic imaging of changing image contrasts, like in T_1 or T_2 mapping.[33]

After the complete reconstruction of the measurement, a principle component analysis (PCA) was performed on the data set in the image plane. Optimally, the first principal components contain the image information, higher components contain noise. By cutting off higher components, noise in the image can be reduced and the image quality improved. It is not possible to reduce MRI-induced artefacts because they are contained in the image and are not normal distributed noise.

Capturing the motion of the TMJ relies on a rapid imaging method to avoid blurring artefacts. However, a frame requires a sufficient time span; hence, a radial sampling pattern was utilized.

To obtain dynamic images, the measured data set was reconstructed offline with Matlab (MathWorks, Natick, MA). Notably, all post-processing algorithms could potentially be implemented in the control computer of the MRI system, so that the examiner can eye the videos immediately after the measurement. Post-processing of the data was achieved by a sequence comprising gridding, sliding window or KWIC filter selection, a fast Fourier transform and, optionally, a PCA.

The parameters of the reconstruction, such as number of spokes, view sharing, principal components, were tuned to receive an adequate balance in signal-to-noise ratio (SNR), temporal resolution and spatial resolution. For one frame, 34 projections were used for the sliding window reconstruction, which corresponds roughly to a time window of 0.68 s. When using the KWIC filter, constant Nyquist sampling was chosen.

To quantify the intra-articular space, the voxels were counted.

After reconstruction, the animations were viewed by a clinician and analysed for irregularities of anatomical structures with emphasis on the articular disc, the condyle and changes of the intra-articular space.

Results

A total of 22 informed and consenting subjects were examined resulting in data sets, each containing radial dynamic data from the two joints. All measurements were well tolerated by the subjects. The average time demand of a dynamic TMJ examination was roughly 5 min.

MR images of the TMJ before and after a PCA reconstruction are shown in Figure 3. The PCA filtering process increases the SNR of the images and lead to a more precise interpretation of the joint's structures. Outtakes of dynamic imaging of a healthy joint's kinematics are shown in Figure 4. The dynamic image sequence displays selected images taken from one opening

Figure 3 Before and after performing a principle component analysis. A considerable amount of noise could be removed from the image, and the boundaries of the structures become better delineated

and closing cycle. The condyle and the fossa are delineated sharply, the disc (arrow) is visible in the images owing to the chosen echo time of TE = 12 ms. The disc slides along normally during the opening movement of the condyle (images from the closing movement are not shown).

In Figure 5, a comparison is made between the kinematics of one subject's TMJ at given points in time. The sequence displays closing movement of the joint with (left) and without (right) masticatory loading. Under load, the condyle is depressed farther into the fossa during terminal occlusion (left). In these images, the disc is not always directly visible owing to a TE of 5 ms. However, the intra-articular distance provides sufficient information about the size and localization of the disc.

An examination performed with the proposed method revealed reasons behind painful symptoms experienced by one subject, diagnosed with TMD beforehand, where conventional diagnostics had not yielded conclusive results able to explain the patient's condition. In this case, pain and clicking only occurred under unilateral loading nearing the closed-mouth position. No pain was felt when an unloaded closing motion was performed. Although X-ray imaging indicated a deformed articular disc, it was not until the dynamic MRI methods were applied that it was found that the disc was displaced in front of the condyle under masticatory loading. When the terminal position was reached while chewing, the disc was compressed between the condyle and the rear portion of the articular fossa. Figure 6 illustrates the differences in the joint space under unloaded (left) and loaded (right) conditions. The imaging parameters in the static measurement are chosen equally to the dynamic to obtain a comparable accuracy.

Discussion

The goal of this study was to develop and evaluate a fast dynamic MRI technique for measurement of the TMJ's

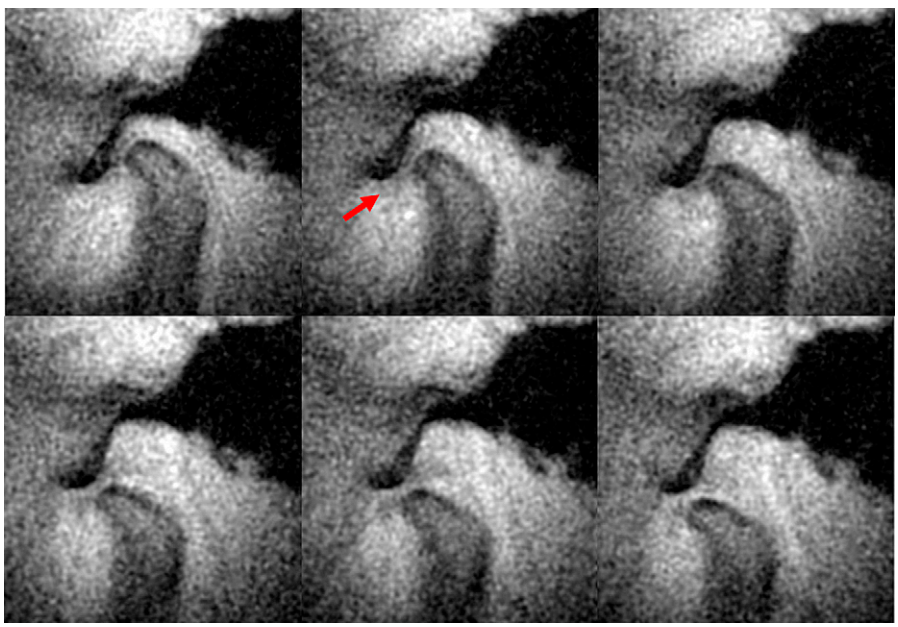

Figure 4 Exemplary image series of a healthy joint (right side) during opening of the mouth. The mouth is (upper left) closed at the beginning of the measurement and wide open (bottom right) at the end. The physiological movement of the disc in the intra-articular space is visible (arrow). The series is reconstructed using the k-space-weighted image contrast filter at constant Nyquist sampling

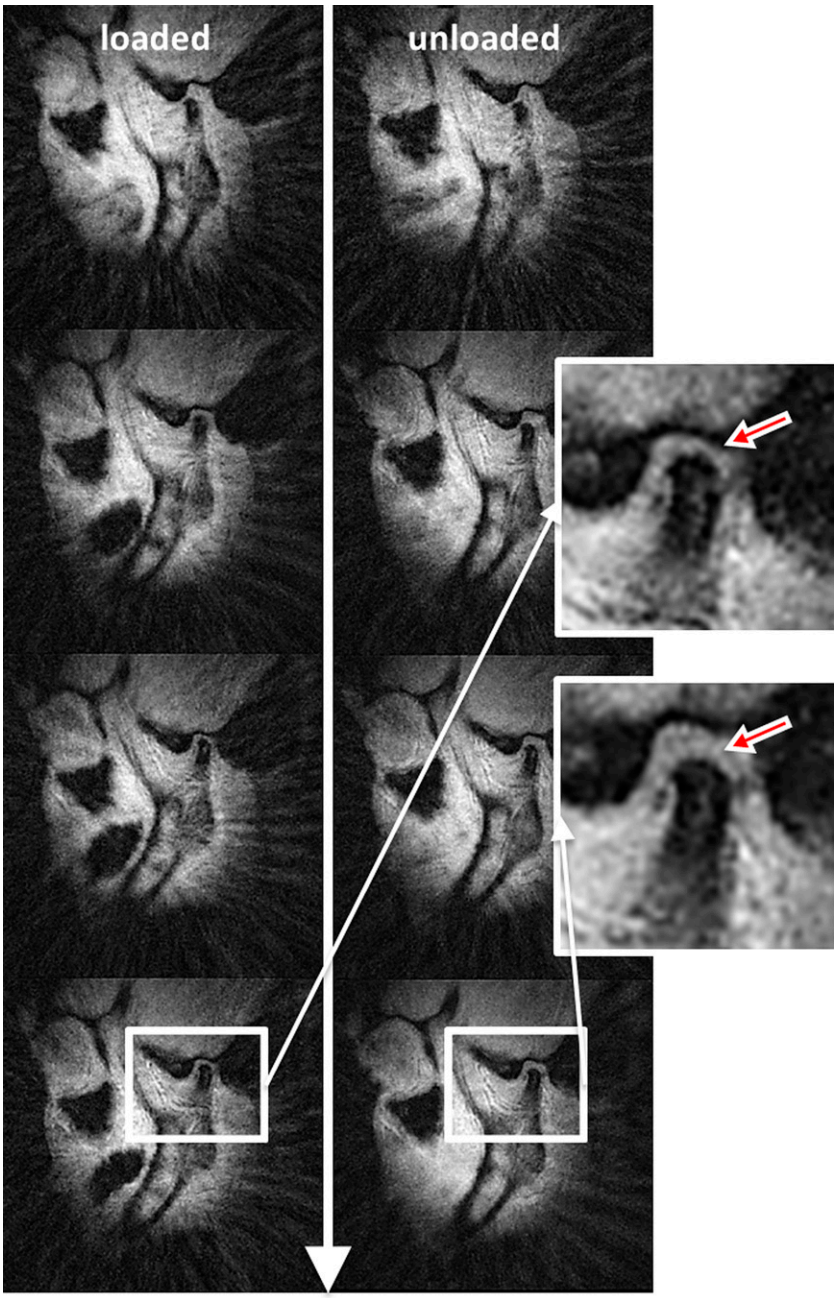

Figure 5 Right temporomandibular joint during an ipsilateral loaded (left) and unloaded (right) closing movement of the jaw. At the end of the series terminal occlusion is reached. While biting on candy, the cartilage in the intra-articular space is more compressed than in the unloaded state

motion with an arbitrary reconstruction window time point and width, which would extend the work by Chen et al[18] and Shimazaki et al[19] by providing real-time dynamic measurements. The proposed method allows for choosing the optimal trade-off between spatial and temporal resolution after the measurement and does not require any *a priori* knowledge about the expected motion kinetics.

Axiographic methods are able to track the mandibular motion in submillimeter resolution, yet it is not easily possible to examine the loaded joint owing to the need to fasten a tray with tracing markers to the mandible. With the method described here, loading is achieved by chewing on a cooled caramel toffee, which does not interfere with the measurement method. The proposed technique combines the advantages of axiography (condyle movement) and static imaging (visibility of soft tissue) under physical load condition, particularly relevant for subjects claiming pain while chewing. Additionally, the data are acquired with little effort in contrast to

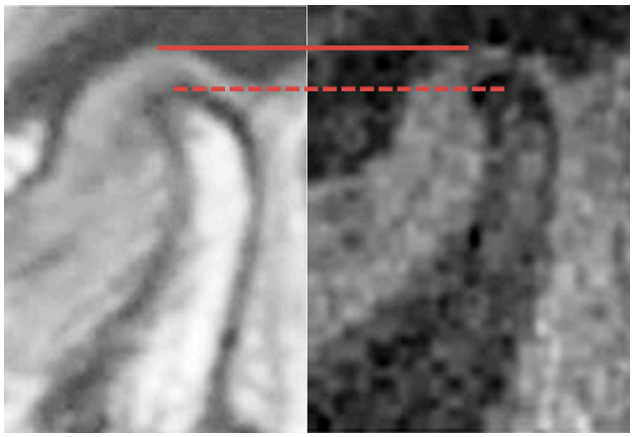

Figure 6 The MR image on the left-hand side shows a static measurement of the temporomandibular joint with imaging parameters comparable with the dynamic measurement. On the right-hand side, the last image of a dynamic series of the same joint in terminal occlusion under loading is shown. The deepest point of the fossa is marked with a line, whereas the dotted and dashed lines indicate the topmost point of the condyle. Note the different distances

axiography, as in most cases, TMD patients undergo (static) MRI examinations anyway.

The radial trajectory is suitable for dynamic and rapid imaging because the k-space is adequately covered with only few projections. The Nyquist criterion determines the amount of sample points in k-space per area unit. Sensitive low frequency information that contains most of the image contrast is found in the centre of the k-space, and in the case of radial imaging, the Nyquist criterion for this part of the k-space is fulfilled with only a few projections. Classic Cartesian sampling allows a relatively high resolution but comes with the drawback of long acquisition time (TA), rendering this method unsuitable for moving objects.

Echo planar imaging represents a very fast Cartesian imaging method, where the complete frequency space is sampled within one pulse shot. Echo planar imaging sampling substantially shortens TA, albeit by a margin still not enough to capture rapid motions as they occur in the TMJ, resulting in strong motion and undersampling artefacts.

By contrast, radial data sampling techniques[34] are based on the principle of measuring projections (spokes) that all cross the centre of the k-space under a certain angle. Accordingly, they provide a substantially faster method to obtain enough data material for an image reconstruction, at a marginal cost of image quality which is only impaired by blurring and streaking caused by motion and intentional undersampling.[35,36] These artefacts are less distinct than the severe aliasing that occurs in undersampled Cartesian imaging.

In this study, susceptibility and metal artefacts arising from dental filling materials were not obstructive. In one case, a retainer produced pronounced artefacts, but it did not affect the imaging of the TMJ and its surroundings.

Using the properties of PCA, it is possible to reduce the amount of noise in a single time frame; however, noise in subsequent time frames is then no longer uncorrelated. This makes it easier for the clinician to estimate the intra-articular space (Figure 4). Then again, the PCA contributes to slightly increased motion artefacts because the motion during the measurement is interpreted as noise. By tuning parameters reasonably, PCA improves image clarity.

Decreasing the size of the reconstruction window reduces the amount of data for reconstructing a frame, leading to a lower SNR. However, a higher time resolution is achieved, resulting in less motion blurring of condyle. By reducing noise in the image with the help of PCA, SNR can be slightly improved again.

In conclusion, the method described in this paper could provide additional information to the clinician as it allows monitoring of the TMJ under conditions that are invisible with current technologies. A dynamic imaging method in combination with loading of the TMJ was demonstrated in this study. As this study concentrated on the imaging potential of radial dynamic MRI of TMJ in different load states, only qualitative comparison between healthy joints and those marred with TMD has been made. If this technique is capable of revealing TMD, clinical trials should be carried out expanding the scope to quantitative measuring, lastly rendering possibility for therapy planning and monitoring. Further investigations concerning comparison with other methods would also be beneficial.

References

1. Scrivani SJ, Keith DA, Kaban LB. Temporomandibular disorders. *N Engl J Med* 2008; **359**: 2693–2705. doi: 10.1056/NEJMra0802472
2. Okeson JP, Bell WE. *Bell's orofacial pains.* Chicago, IL: Quintessence Publishing; 1995.
3. Suma S, Veerendra Kumar B. Temporomandibular disorders and functional somatic syndromes: deliberations for the dentist. *Indian J Dent Res* 2012; **23**: 529–536. doi: 10.4103/0970-9290.104965
4. Rues S, Lenz J, Türp JC, Schweizerhof K, Schindler HJ. Muscle and joint forces under variable equilibrium states of the mandible. *Clin Oral Investig* 2010; **15**: 737–747. doi: 10.1007/s00784-010-0436-4
5. Iwasaki LR, Crosby MJ, Gonzalez Y, McCall WD, Marx DB, Ohrbach R, et al. Temporomandibular joint loads in subjects with and without disc displacement. *Orthop Rev (Pavia)* 2009; **1**: 90–3. doi: 10.4081/or.2009.e29
6. Tuijt M, Koolstra JH, Lobbezoo F, Naeije M. Differences in loading of the temporomandibular joint during opening and closing of the jaw. *J Biomech* 2010; **43**: 1048–1054. doi: 10.1016/j.jbiomech.2009.12.013
7. Huddleston Slater JJR, Visscher CM, Lobbezoo F, Naeije M. The intra-articular distance within the TMJ during free and loaded closing movements. *J Dent Res* 1999; **78**: 1815–1820.
8. Tymofiyeva O, Proff P, Richter E-J, Jakob P, Fanghäenel J, Gedrange T, et al. Correlation of MRT imaging with real-time axiography of TMJ clicks. *Ann Anatomy* 2007; **189**: 356–361. doi: 10.1016/j.aanat.2007.02.009

9. Wagner A, Seemann R, Schicho K, Ewers R, Piehslinger E. A comparative analysis of optical and conventional axiography for the analysis of temporomandibular joint movements. *J Prosthet Dent* 2003; **90**: 503–509. doi: 10.1016/S0022391303004827
10. Lückerath W. Differential diagnosis of electronic TMJ tracings in dysfunction patients. *Dtsch Zahnarztl Z* 1991; **46**: 722–726.
11. Hansson LG, Westesson PL, Katzberg RW, Tallents RH, Kurita K, Holtås S, et al. CT and MR of the temporomandibular joint: comparison with autopsy specimens made at 0.3 T and 1.5 T with anatomic cryosections. *AJR Am J Roentgenol* 1987; **148**: 1165–1171.
12. Larheim TA. Current trends in temporomandibular joint imaging. *Oral Surg Oral Med Oral Pathol Oral Radiol Endod* 1995; **80**: 555–576.
13. Westesson PL. Reliability and validity of imaging diagnosis of temporomandibular joint disorder. *Adv Dent Res* 1993; **7**: 137–151.
14. Emshoff R, Gerhard S, Ennemoser T, Rudisch A. Magnetic resonance imaging findings of internal derangement, osteoarthrosis, effusion, and bone marrow edema before and after performance of arthrocentesis and hydraulic distension of the temporomandibular joint. *Oral Surg Oral Med Oral Pathol Oral Radiol Endod* 2006; **101**: 784–790.
15. Kuroda S, Tanimoto K, Izawa T, Fujihara S, Koolstra JH, Tanaka E. Biomechanical and biochemical characteristics of the mandibular condylar cartilage. *Osteoarthritis Cartilage* 2009; **17**: 1408–1415. doi: 10.1016/j.joca.2009.04.025
16. Singh M, Detamore MS. Biomechanical properties of the mandibular condylar cartilage and their relevance to the TMJ disc. *J Biomech* 2009; **42**: 405–417. doi: 10.1016/j.jbiomech.2008.12.012
17. Yamada I, Murata Y, Shibuya H, Suzuki S. Internal derangements of the temporomandibular joint: comparison of assessment with three-dimensional gradient-echo and spin-echo MRI. *Neuroradiology* 1997; **39**: 661–667.
18. Chen Y-J, Gallo LM, Meier D, Palla S. Dynamic magnetic resonance imaging technique for the study of the temporomandibular joint. *J Orofac Pain* 2000; **14**: 65–73.
19. Shimazaki Y, Saito K, Matsukawa S, Onizawa R, Kotake F, Nishio R, et al. Image quality using dynamic MR imaging of the temporomandibular joint with true-FISP sequence. *Magn Reson Med Sci* 2007; **6**: 15–20.
20. Zhang S, Block KT, Frahm J. Magnetic resonance imaging in real time: advances using radial FLASH. *J Magn Reson Imaging* 2010; **31**: 101–109.
21. Zhang S, Gersdorff N, Frahm J. Real-time magnetic resonance imaging of temporomandibular joint dynamics. *Open Med Imaging J* 2011; **5**: 1–7.
22. Lauterbur PG, Lai C-M. Zeugmatography by reconstruction from projections. *IEEE Trans Nucl Sci* 1980; **27**: 1227–1231.
23. Haacke EM, Brown RW, Thompson MR, Venkatesan R, Cheng N. *Magnetic resonance imaging: physical principles and sequence design.* New York, NY: John Wiley & Sons, Inc.; 1999.
24. Paschal CB, Morris HD. K-space in the clinic. *J Magn Reson Imaging* 2004; **19**: 145–159. doi: 10.1002/jmri.10451
25. Bracewell R. *The Fourier transform and its applications.* New York, NY: McGraw-Hill Science/Engineering/Math; 1999.
26. Twieg DB. The k-trajectory formulation of the NMR imaging process with applications in analysis and synthesis of imaging methods. *Med Phys* 1983; **10**: 610–621.
27. Rasche V, De Boer RW, Holz D, Proksa R. Continuous radial data acquisition for dynamic MRI. *Magn Reson Med* 1995; **34**: 754–761.
28. Winkelmann S, Schaeffter T, Koehler T, Eggers H, Doessel O. An optimal radial profile order based on the golden ratio for time-resolved MRI. *IEEE Trans Med Imaging* 2007; **26**: 68–76. doi: 10.1109/TMI.2006.885337
29. Brigham OE. *FFT—schnelle Fourier-transformation.* Munich, Germany: R. Oldenbourg; 1995.
30. Jackson JI, Meyer CH, Nishimura DG, Macovski A. Selection of a convolution function for Fourier inversion using gridding. *IEEE Trans Med Imaging* 1991; **10**: 473–478. doi: 10.1109/42.97598
31. Fessler JA. Nonuniform fast Fourier transforms using min-max interpolation. *IEEE Trans Sig Proc* 2003; **51**: 560–574.
32. Song HK, Dougherty L. Dynamic MRI with projection reconstruction and KWIC processing for simultaneous high spatial and temporal resolution. *Magn Reson Med* 2004; **52**: 815–824. doi: 10.1002/mrm.20237
33. Song HK, Dougherty L. k-Space weighted image contrast (KWIC) for contrast manipulation in projection reconstruction MRI. *Magn Reson Med* 2000; **44**: 825–832.
34. Lauterbur PC. Image formation by induced local formations: examples employing nuclear magnetic resonance. *Nature* 1973; **242**: 190–191.
35. Lauzon ML, Rutt BK. Polar sampling in k-space: reconstruction effects. *Magn Reson Med* 1998; **40**: 769–782.
36. Vigen KK, Peters DC, Grist TM, Block WF, Mistretta CA. Undersampled projection-reconstruction imaging for time-resolved contrast-enhanced imaging. *Magn Reson Med* 2000; **43**: 170–176.